DEMI (Debris Elimination and Management Instrument)

Leon Aharonian, Nicolas Aldana, Miles Huntley-Fenner, Yidi Reiss, Christina Wright

DEMI

The authors are with the Department of Mechanical Engineering, Columbia University, New York, NY (la2807@columbia.edu, na2851@columbia.edu, mnh2130@columbia.edu, lr3057@columbia.edu, cmw2232@columbia.edu). This material is based upon work developed in the MECE E3420 / E3430 Engineering Design Courses

***Abstract*— DEMI (Debris Elimination and Management Instrument): A novel solution for space debris removal. Space debris poses a serious threat to the safety and sustainability of orbital activities. To address this challenge, we designed DEMI, a collection mechanism that can capture and store multiple pieces of small debris in low Earth orbit (LEO). DEMI works with a two stage capture system: an outer aperture that encloses the debris, and an inner door that seals it inside a storage chamber. DEMI can be easily attached to the ESPAStar satellite bus, which provides the necessary power, propulsion, and communication systems. DEMI is made of space grade aluminum with the ability to add shielding to withstand the harsh environment of LEO.**

I. Introduction

The accumulation of space debris in LEO is a growing threat to the safety and sustainability of our daily lives. Thousands of trackable space debris larger than 10 centimeters in width may collide with satellites and spacecraft, breaking them into smaller pieces of debris and creating a cascade effect known as Kessler Syndrome. Each collision results in the increased likelihood of further collisions. This could disrupt or destroy services such as GPS, internet, television, weather monitoring, and emergency response. Additionally, since free-moving space debris is unpredictable and uncontrollable, it may harm people and property on Earth upon atmospheric reentry. Current solutions include a harpoon to spear a cube-sat[1], a net to envelop the target[2], or custom built claws to target one specific piece of debris [3]. However, all of these could potentially cause more debris to form upon the collision of the debris with the collector and all of them are single use. Other solutions propose equipping all future satellites with standardised magnetic docking ports[4] or drag sails[5] to ease their retrieval but this doesn't help the current situation. Thus, there is currently no cost-effective method to collect or destroy space debris and prevent further damage to the space environment.

The Debris Elimination and Management Instrument (DEMI) is a prototypical reusable space debris collection system designed to clean Earth orbit of this potentially harmful material. It operates through the use of an airlock system. Debris is initially captured in a quarter-cylinder and flap clamshell which sits atop a secondary set of garage-style doors. Once debris is secured in the cylinder, the doors open, and the flap pushes debris through the newly formed opening. The doors then close, safely storing the space junk below our mechanism and allowing the outer clamshell to reset for more debris. DEMI was designed to be self-contained and non-intrusive to enable interface with existing space infrastructure and modular satellite bus systems.

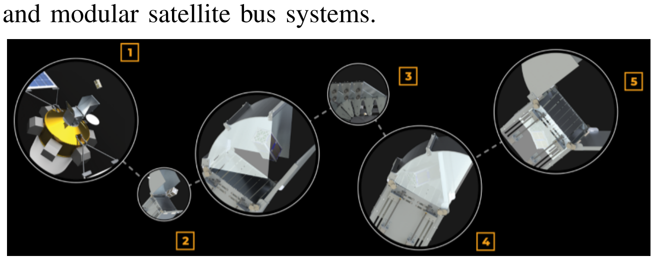

Fig. 1. The capture sequence

The major design constraints of this mechanism fall into four categories: size, material, mission architecture, and manufacturability. The size of the physical mechanism is limited by a desire to minimize launch volume and maximize effectiveness at capturing space debris of the target size. The material of the mechanism must be strong enough to withstand several collisions, suitable for the harsh temperatures of space, and lightweight so that it may be a reasonable payload mass for a rocket.

The mission architecture provided another set of constraints. First, the approach. The mechanism must be able to both capture and contain multiple pieces of space debris–during a capture attempt, it was crucial to ensure that the stored space debris would not have an opportunity to escape from the storage mechanism. An ideal mechanism would also be reusable and compatible with existing space infrastructure.

The final design constraint is manufacturability. The resultant mechanism must be sufficiently mechanically complex to be novel, but feasible to manufacture given the available time and machinery. An ideal mechanism would be as simple as possible and minimize complex geometry.

II. Methods

A. Size

The targeted space debris has a size of 10 to 30 centimeters. This range was chosen for three reasons: one, debris of this size is the smallest trackable size; two, there is no current space debris removal solution that targets debris within this size range; and three, a larger size range of debris would likely require a more resource-intensive solution that would be infeasible to manufacture within the scope of our project. 10 to 30 centimeters is a comfortable balance between feasibility and relevance to the defined problem.

The mechanism needed to comfortably fit any piece of debris within that range, so it was decided that each side should have at least 5 centimeter of clearance. DEMI's inner aperture is designed to have a width of 40 centimeters, while the outer aperture has a radius of 40 centimeters. This should allow any piece of debris within the target size to be captured without risk of jamming.

B. Material

Due to its low relative weight, durability, and cost-effectiveness, 1/8" T6 6061 aluminum was the metal of choice for most parts. Finite element analysis (FEA) was conducted as discussed in section F to test if the material properties of aluminum were suitable for the types of impacts and collisions DEMI would normally experience.

As the analysis in section F indicates, aluminum is an appropriate choice of metal, and the addition of kevlar reinforcement may help to significantly extend DEMI's mission lifespan.

C. Approach

The two priorities given by the mission scope were reusability and reliability. Thus, DEMI's two-stage capture design was adopted. In this design, an outer aperture is responsible for sealing the space debris, while an inner set of doors enables independent opening and closing of the storage chamber.

Fig. 2. Outer enclose of DEMI in the Closed configuration. A piece of debris is captured between the quarter cylinder and the flap.

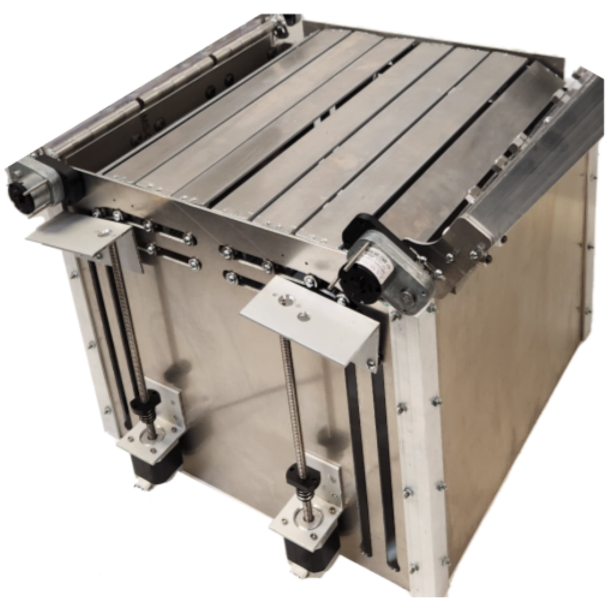

Fig. 3. DEMI's inner enclosure in the closed position.

This design choice effectively addresses the reusability constraint, as the capture method itself is not limited in terms of the number of captures it can perform. Instead, the capacity of the storage chamber becomes the primary limitation, as it provides a finite space for accommodating the captured debris. This approach ensures both reliability and reusability while still adhering to the constraints of the mission.

Since mission-specific constraints, such as propulsion systems, computer vision, or power, are outside of the scope of this project, DEMI is currently designed to be compatible with existing space infrastructure. DEMI is intended for use with Northrop Grumman's ESPAStar bus, a modular space infrastructure resource for hosting operational payloads. The ESPAStar is an appropriate choice of infrastructure given its suitability for multi-year missions.

Fig. 4. Northrop Grumman's ESPA Star. An of the shelf space bus.

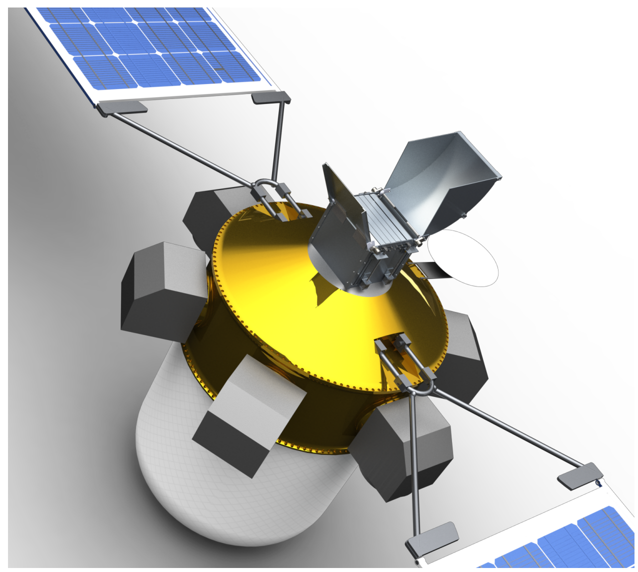

Fig. 5. DEMI mounted on ESPA Star.

D. Manufacturing

Given the time, material, and budget constraints for this project, one of the primary concerns was manufacturing. It is infeasible to manufacture and test a design more reminiscent of existing space debris removal missions with the tools available. Therefore, we avoided complex geometries and focused on meeting the other design constraints discussed earlier. DEMI was designed for the majority of its parts to be machined out of 1/8" or 1/4" inch aluminum sheet metal. Other parts, such as screws or bearings, were off-the-shelf, with a select few (ex: motor mounts) requiring more processing. Designing with manufacturability in mind allowed for a faithful prototype of DEMI to be built within five months without exceeding the allocated budget.

E. ***Outer Motor Selection***

Solidworks motion studies were performed to determine necessary motor torque to actuate the clamshell and flap via direct drive in a microgravity environment. An assembly of the box, flap, and cylinder was fitted with a hypothetical motor at the cylinder hinge, which was given instructions to rotate in a 70 degree arc over the course of 30 seconds. The incremental torque values required by the motor were exported, then graphed. Motors were selected on the basis of this analysis.

F. Inner Motor Selection

To select motors, the constraints to actuate the inner doors were determined. High precision was necessary, however speed was a non factor. Options like belts or cables were removed as they had additional levels of complexity that were deemed unnecessary. Stepper motors with lead screws were selected due to their high precision and attachment requirements. An equation was used to determine how much power was needed out of the motor, relating the geometry of the lead screw, the motor ratings and the relevant materials to determine the maximum force F that could be delivered by the motor. This relationship is given by Eq. (1) which was found from [6].

$$F = \frac{2T_R}{d_m} * \frac{\pi * d_m - f * l * sec(\alpha)}{l + \pi * f d_m sec(\alpha)} \tag{1}$$

In Eq. (1), T_r is the stall torque of the motor, d_m is the average diameter of the lead screw, f is the coefficient of kinetic friction between the lead screw and the nut, l is the vertical distance between threads and alpha is the angle between the horizontal and the thread surface.

The weight of each of the inner doors was determined within Solidworks by assigning relevant materials to the assembly and having the software calculate the total weight of each door.

G. Finite Element Analysis - Impact Analysis

In order to obtain the force and stress values experienced by DEMI, an impact analysis needed to be performed. However, a worst case reasonable scenario needed to be understood in order to perform the impact analysis. A collision with a half density, 30cm diameter sphere was chosen. 30cm is the largest diameter of debris DEMI was designed to capture and aluminum is the most commonly used material in space [7]. The 50% infill value was chosen because there are no solid aluminum spheres floating in space and it was determined, together with NASA JPL, that this would be the most representative estimate. However, a semi hollow sphere may behave unpredictably in simulation, so a smaller, solid sphere with the same mass as a 50% density, 30cm sphere of aluminum was chosen. This represents the worst case impact scenario. The proper diameter for this smaller sphere was found via equation (2).

$$\begin{gathered} \frac{1}{2} * \frac{3}{4} * \pi(15^3) = \frac{3}{4} * \pi(r^3) \\ \implies r = \sqrt[3]{\frac{1}{2}(15^3)} \implies r = 11.9055cm \end{gathered} \tag{2}$$

In order to determine the speed of the collision in this worst case realistic scenario, current and historical docking operations were studied. It was found that the space shuttle docked to the International Space Station with a relative velocity of 0.03125m/s [8]. However, a speed of 10 times that of the shuttle (0.3 m/s) was used as the worst case scenario. This was done because the debris momentum was much lower compared to that of a docking space shuttle, and human comfort, which is better served by slower speeds, was not a priority. Furthermore, fuel economy could be maximized with a minimal decrease in speed.

The center of one of the $1/8$ inch thick garage door sections was chosen as the impact point. This was chosen because it was the furthest from any supports making it the worst case scenario. With all the constraints chosen, an FEA study was prepared in LS-PrePost. A simplified garage door section (the impact section) without the mounting holes was created because there were issues with importing SolidWorks models into the software. Therefore, both the sphere and the impact section were created as solid meshes in LS-PrePost. The nodes on the left and right ¼ inch of the impact section were constrained in place to simulate the connection of the sections to the bearing attachment pieces as seen in figure 7.

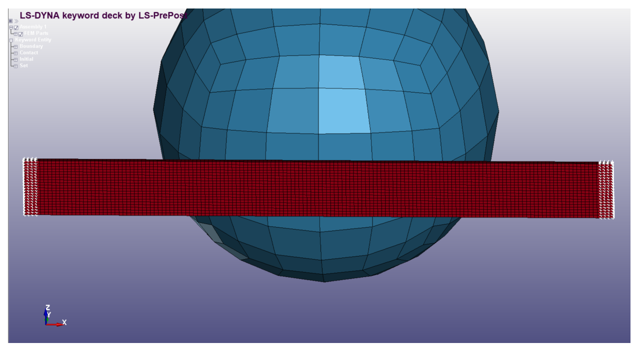

Fig. 6. This image shows the constraints applied to the impact section.

For the analysis software, Ansys LS-DYNA was used primarily due to its capability to simulate the response of materials to short periods of severe loading [9]. A consistent unit system was required by the software, and the system of mm, ms, and kg was chosen due to the size and timescales applicable. Through a unit conversion, this led to stress units of GPa (10^9Pa), force of $10^3 N$, and a density of kg/mm^3. This meant that the material properties needed to be input accordingly. It was found that for T6 6061 Aluminum, the density was $2.700 * 10^{-6} kg/mm^3$, the Young's modulus 69.95GPa, and the Poisson Ratio was 0.33 [10]. These properties were entered in the 001_ELASTIC material option and were used both for the sphere and the impact section. As for the contact type, the AUTOMATIC_SURFACE_TO_SURFACE option was used, with the sphere as the slave component and the impact section as the master.

After the relevant selections were made to set up the simulation, a termination time of 100 ms was chosen (which was enough to cover the full collision event), with a 0.01ms time step between data points. This simulation was run 3 times with ever smaller mesh elements on the impact section and mesh convergence was tested. The mesh on the sphere was not changed because it would have added computation time with no added value as the purpose was to see the response of the impact section and not the sphere.

III. Results

A. Calculated Results

1) Outer Motor: The maximum required torque was found to be 0.02 kg*cm, which was then used to motivate the decision of which motors to buy. The assumption was that any motor powerful enough to actuate the cylinder would also be powerful enough to actuate the flap, therefore the baseline of 0.02 kg*cm was used in the motor selection for both cases. A 3865SG-520-0630-125 Micro Flat Spur Gear Motor with 3 kg*cm of torque was chosen on the basis of this analysis. It was fairly inexpensive ($10.98) and the wide torque margin helped us to account for unknown values such as friction in the hinges.

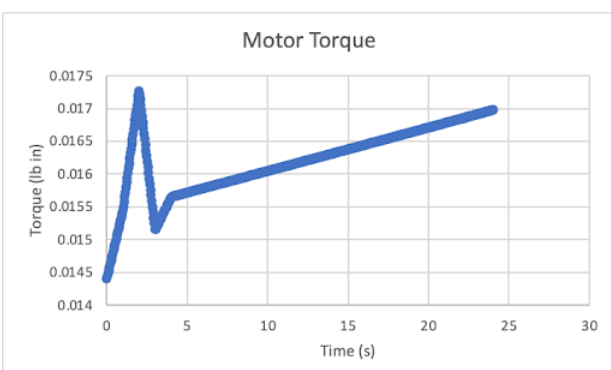

Fig. 7. This image shows the motion study data for the outer motors.

2) Inner Motor: We applied Eq.(1) to the NEMA 17 Iverntech Motor with a T8 lead screw. The values used were as follows: T_r was 500 mNM, f was .19, l was 2.0 mm, d_m is 7.1 mm and α is 14.5°[11], [12]. We found the maximum force that could be delivered by this motor with our selected lead screw and nut at maximum power to be 120 newtons. The mass of each inner door was found to be 1.35 kg, requiring a minimum of 13.5N to lift.

3) Impact: After performing the analysis discussed in section F above, the Von Mises Stress results were obtained and placed in figure 8.

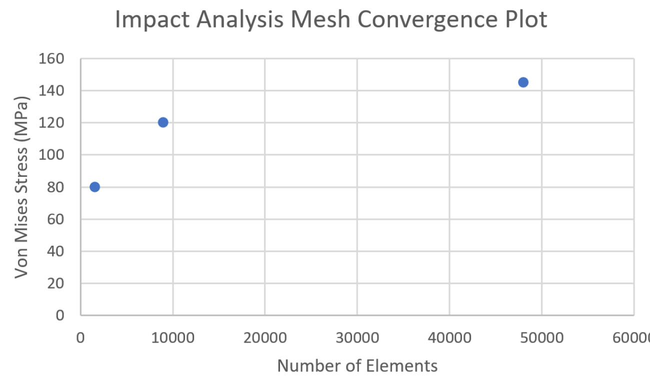

Fig. 8. This plot shows how the Von Mises stress converges as the number of elements increases.

The reaction force and the displacement plots can be found in figures 9 and 10 respectively.

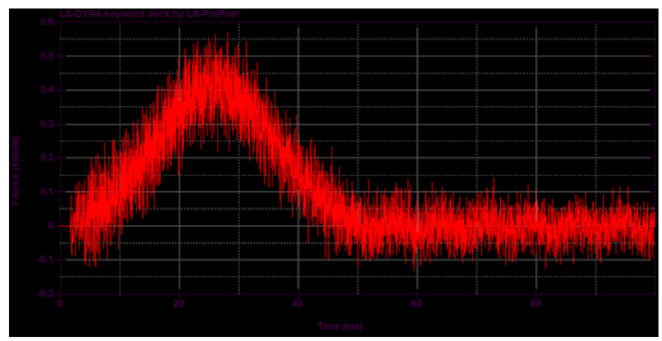

Fig. 9. This plot shows the Y-Axis reaction force in $10^3 N$ throughout the collision.

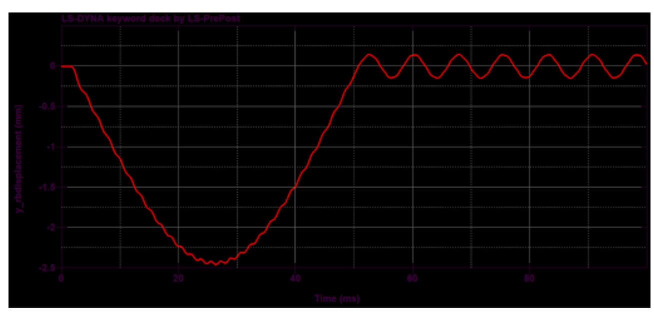

Fig. 10. This plot shows the Y-Axis displacement in mm throughout the collision.

Lastly, the visuals of the whole top section, bottom center, and top edge of the impact section at the time of maximum stress can be seen in figures 11, 12, and, 13 respectively, with the color scale in GPa shown in figure 14.

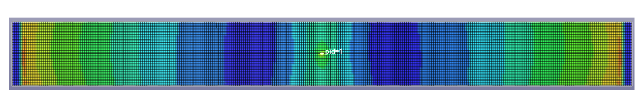

Fig. 11. This visual shows the Von Mises stress concentrations at the moment of max stress on the top side of the impact section.

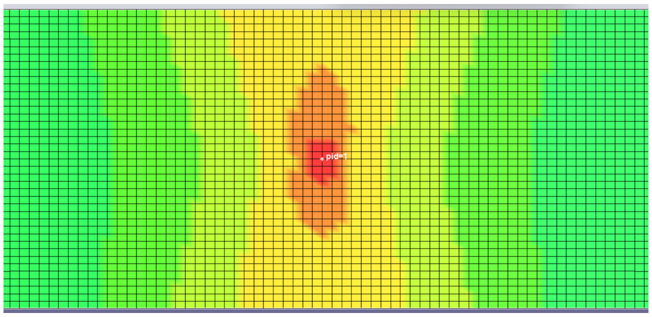

Fig. 12. This visual shows the Von Mises stress concentrations at the moment of max stress on the bottom center of the impact section.

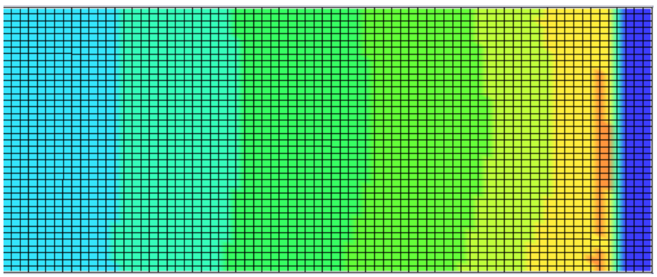

Fig. 13. This visual shows the Von Mises stress concentrations at the moment of max stress on the top edges where the section is constrained.

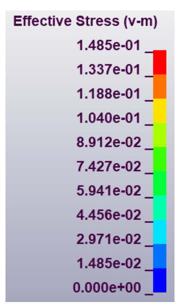

Fig. 14. This chart shows the correlation between the colors from figures 11 - 8, and the Von Mises stress in units of GPa.

IV. Discussion & Conclusion

A. Interpretation of Results

1) Inner Motors: From Eq.(1) we determined that the maximum force that can be delivered by our selected motors is 120N. With each inner door requiring a minimum of 13.5 N to lift and two motors on each door, the motor selection will be fully adequate to control the doors on earth. In zero gravity, the doors will require even less force, only needing to overcome friction. Though the motors deliver 17x the required force, the NEMA 17 was selected due to it's availability and ease of use over smaller motors, which would have required us to create our own lead screw apparatus.

The main shortcoming in this analysis was only looking at the force delivered by the motor without considering friction from the motion of the mechanism. In practice, it was observed that the doors jam at high speeds, indicating further analysis should be conducted to include friction between the bearings and the track in the force calculations.

2) Outer Motors: With the mechanism placed on its side and fully supported with standoffs, the effects of gravity were sufficiently negated to allow the outer motors to function as predicted by the motion study analysis. The torque margin proved significant enough to overcome the friction in the hinges, and ultimately supported much higher speeds than had been simulated. The cylinder was able to close in 2 seconds - which far exceeded the 30 seconds which had been simulated. The Flap had a closing time of 3 seconds.

3) Impact: From figure 8 we clearly see that the Von Mises stress converges at $< 150MPa$. This is significantly below the material's tensile yield strength of 276MPa [10] and provides us with a factor of safety > 1.8 which is above NASA's required FOS for Yield of 1.0 for our use case [13]. This showed us that our material and thickness of choice for the garage door section was adequate. We also found a peak reaction force of $\approx 600N$ and displacement of $\approx 2.5mm$ as seen in figures 9, and 10 respectively. From these plots one can see that there is a large initial reaction force and displacement, causing the whole impact section to oscillate back and forth. Columbia University resident FEA expert, professor Kristin Myers said that the material response and fringe plots look exactly how she would expect, and that the analysis seems accurate.

As discussed, the impact section was the worst case scenario and the most likely point of failure. After the impact section, the load splits and a thicker piece of aluminum (¼ inch) is used to connect to the bearings, where the load is distributed further with all parts $> 1/8$ inch perpendicular to the force. This led to us to decide not to propagate the force further and not to perform any FEA on parts further downstream.

The main shortcoming of our analysis was that the impact section was modeled without the mounting holes, and thus did not have the most accurate boundary conditions. Therefore, there is a possibility that the more localized boundary conditions created by the bolts would lead to a higher peak stress than was simulated. In addition, our analysis did not extend to fatigue. Our mission will be experiencing hundreds of collisions during its duration, so fatigue is a major consideration. It is possible that by doing fatigue simulations we would see that the part will fail before the mission is complete. Lastly, our analysis did not account for stress caused by the extreme thermal cycling that DEMI would undergo. This stress could theoretically cause material failure, as well as jamming. The remedy for all of these issues may be to add layers of insulation and Kevlar linings, however we did not have the capability to perform such simulations.

While the analysis done was not perfect, as we have discussed we believe that it was adequate to prove the the resilience of DEMI throughout it's mission duration. However, to gain the utmost confidence in the mission, we would recommend that thermal, fatigue, and higher fidelity model analysis should be completed prior to the mission.

B. Space-Worthiness

Space-worthy motors must be able to function from -196 to 128 degrees Celsius for long periods of time without breaking [14]. To increase our technology readiness level, we would have to purchase motors which are specifically rated to operate over that temperature range. Additionally, the motors and hinges should be lubricated with low-volatility, thermally stable lubricants which possess minimal out-gassing potential [15]. Silicone grease, krytox, and molybdenum disulfide grease are all options which have seen use in aerospace applications. All of these qualities would need to be verified through thermal vacuum chamber testing to mirror the environment found in space.

DEMI would also have to be coated in Kevlar to protect against impacts from space debris. Physical impact testing would have to be conducted to identify the correct weave and thickness of kevlar layer(s). Multi-layer insulation (MLI) consisting of Aluminized Mylar would be placed over the kevlar to provide thermal insulation for the electronics. MLI consists of many layers of reflective material designed to minimize exposure of its contents to radiation. These layers are typically spaced to minimize conduction [16]. Kapton gold or black film would likely be used on the exterior for additional thermal protection, however this decision would need to be verified through thermal vacuum chamber and radiation testing.

Once these improvements have been implemented, the complete system would need to be integrated with a bus, such as the ESPAStar and subjected to a closeout test inside of a thermal vacuum chamber with a coldfinger. This would verify that everything is working properly and minimize out-gassing potential once in space.

C. Comparison to Literature

Unlike the existing methods for clearing debris from LEO discussed in I, DEMI is able to reliably capture many pieces of debris in one mission. Because the captured debris is contained within solid walls upon initial contact, there is no possibility for pieces to break off and further threaten our orbital infrastructure. This is a significant improvement upon solutions like the net, harpoon, and claws. Furthermore, unlike solutions for retrieving future satellites, DEMI is able to target the existing debris and can help prevent Kessler Syndrome before it progresses irreversibly.

D. Conclusion

In conclusion, FEA, motion studies, and other calculations were used to empirically motivate design decisions for DEMI, which has fulfilled its simulations and demonstrated the feasibility of the world's first reusable two stage space debris capture system. With additional components, such as Lidar, kevlar, space-worthy motors, and MLI, it would be prepared for mounting to a custom satellite bus for an experimental spaceflight. With enough funding and innovation, Kessler Syndrome might soon be vanquished by a fleet of such devices in the near future. NASA JPL and the professors of the Columbia University Mechanical Engineering Department - particularly Professor Yesilevskiy - were exceedingly helpful in this project, and their contributions should be lauded alongside those of the DEMI team.

REFERENCES

[1] SciNews, "Removedebris's harpoon captures space debris." Online Video, 2019. Accessed: 5/9/23.

[2] SciNews, "Removedebris's net captures space debris." Online Video, 2018. Accessed: 5/9/23.

[3] ClearSpace, "Clearspace-1 approaching the vespa." Online Video, 2023. Accessed: 5/9/23.

[4] Astroscale, "Cosmic - cleaning outer space mission through innovative capture." Online Video, 2023. Accessed: 5/9/23.

[5] SSTLTV, "Removedebris active debris removal demonstration mission." Online Video, 2018. Accessed: 5/9/23.

[6] L. B. Lectures, "Power screws - stepper motor, lead screw, piston - example 1," 2020.

[7] M. M. Finckenor, "6. materials for spacecraft,"

[8] "Math and science at work - educator edition," 2023.

[9] "Ansys ls-dyna," 2023.

[10] A. International, "Aluminum 6061-t6; 6061-t651," 2023.

[11] Inverntech, "Iverntech nema 17 stepper motor with integrated 100mm t8 lead screw for reprap prusa i3 3d printers z axis or cnc machine," 2019.

[12] N. IMS, "Hybrid stepper motor linear actuator lm17 nema 17 1.5 a 1.8° external linear stepper motor."

[13] C. T. Modlin and J. J. Zipay, "The 1.5 1.4 ultimate factors of safety for aircraft spacecraft – history, definition and applications," tech. rep., NASA, 2014.

[14] M. Finckenor, "Environmental conditions for space flight hardware," 2004.

[15] C. E. Vest, "Lubrication of spacecraft mechanisms," 1993.

[16] M. Finckenor, "Multilayer insulation material guidelines," 1999.